JOC The Journal of Organic Chemistry

Article

pubs.acs.org/joc

Photolysis of a Benzyne Precursor Studied by Time-Resolved FTIR Spectroscopy

Joel Torres-Alacan*

Institute for Physical and Theoretical Chemistry, Rheinische Friedrich-Wilhelms-Universtität, Wegelerstraße 12, 53115 Bonn, Germany

Supporting Information

ABSTRACT: The 266 nm laser flash photolysis of phtaloyl peroxide (**2**) in liquid acetonitrile solution at room temperature has been investigated. Upon 266 nm laser irradiation, **2** is effectively photodecarboxylated leading to the formation of *o*-benzyne (**1**) and two equivalents of CO_2, yet a small fraction of photolyzed **2** follows a different pathway leading to 6-oxocyclohexa-2,4-dienylideneketene (**3**) and one equivalent of CO_2. Compound **3** is kinetically reactive and reacts in the microsecond time scale following a first-order kinetic law. The presence of **1** in the photolysis experiment is confirmed by trapping experiments with methyl 1-methylpyrrole-2-carboxylate (**6**). The Diels–Alder reaction between **1** and **6** occurs under the selected experimental conditions on a time scale shorter than 100 ms.

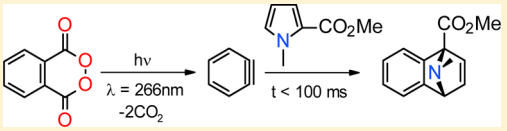

INTRODUCTION

1,2-Dehydrobenzene or *o*-benzyne (**1**) was first proposed as a reactive intermediate in 1927 by Bachmann and Clarke.[1] In the following years, Wittig[2,3] greatly contributed to the understanding of its structure and reactivity. In 1953, Roberts et al.[4] found, in an elegant experiment, that when [1-^{14}C]-chlorobenzene is reacted with potassium amide in liquid ammonia, [1-^{14}C]aminobenzene and [2-^{14}C]aminobenzene are formed in nearly the same proportions. This experiment provided very strong evidence for the existence of **1** as a reactive intermediate in polar liquid phases (Scheme 1). The fascinating history of **1** is the subject of several review articles.[5−7]

Scheme 1

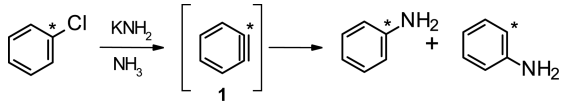

On the basis of the large (37.5 ± 0.2 kcal/mol)[8,9] singlet–triplet energy gap and short (124 ± 2 pm)[10] bond length, **1** is better described as a strained alkyne than as a biradical. Notably, metal complexes containing **1** forming part of the metal coordination sphere have been crystallized, and their structures have been resolved by X-rays.[11−13]

The strained triple bond present in **1** and in arynes in general enables them to participate as reactive intermediates in nucleophilic additions,[14] pericyclic reactions such as Diels–Alder cycloadditions,[15] dipolar cycloadditions,[16] metal-catalyzed[17] reactions, and others.[18] Therefore, it is not surprising that the search for easy-to-handle precursors of **1** still attracts much attention.[19] It is remarkable that more than 75 independent natural products have been synthesized using aryne intermediates.[20] A significant number of those synthetic steps involving **1** or arynes in general proceed with a high degree of regioselectivity. Although useful models able to explain these regioselective trends are emerging,[21] real-time mechanistic studies are still missing.

When it comes to spectroscopy of functional groups, Chapman and co-workers were the first to provide an infrared spectrum of **1** in argon matrices at 8 K by photolysis of phtaloyl peroxide **2**.[22] Chapman and co-workers observed that **1** reacts with furan even at 50 K, forming 1,4-dihydronaphtalene-1,4-endoxide (Scheme 2). In a remarkable work, Radziszewski et al.[23] revisited the IR spectrum of **1** in inert cryogenic matrices and finally located the weak (2.0 ± 0.4 km/mol) C≡C stretching vibration of **1** at 1846 cm^{-1}, which is 120 cm^{-1} less than that previously predicted by theoretical calculations.[24]

Scheme 2. Synthesis and Reactivity of 1 in Argon Matrices

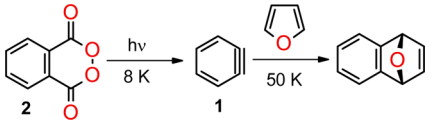

Because **1** is very reactive, the large body of spectroscopic data about it has been collected in the gas[25,26] or solid[10] phase at low temperatures. Spectroscopic data of **1** in liquid solution at room temperature is very scarce. In this regard, the NMR spectra of **1** trapped in the cavity of a hemicarcerand in liquid [D8]-THF measured by Warmuth deserve special mention.[27]

Although much structural and spectroscopic information has been collected on **1**, temporal information is still missing at least in the liquid phase. In this regard, time-resolved spectroscopy, especially with IR detection, has proven to be a

Received: November 23, 2015
Published: January 13, 2016

DOI: 10.1021/acs.joc.5b02678
J. Org. Chem. 2016, 81, 1151−1156

good choice in the study of reactive intermediates and reaction mechanisms.[28−30]

In this paper, I describe a systematic investigation of the photolysis of **2** at room temperature in liquid acetonitrile using time-resolved FTIR spectroscopy. The main goal is to determine whether **1** can be generated from **2** by the action of a single 266 nm photon.

RESULTS AND DISCUSSION

1. UV−Vis Spectroscopy. The electronic spectrum of **2** in acetonitrile at room temperature is located entirely in the UV section, and it is asymmetrically divided into two regions by a shallow minimum around 270 nm (solid curve, Figure 1a). The

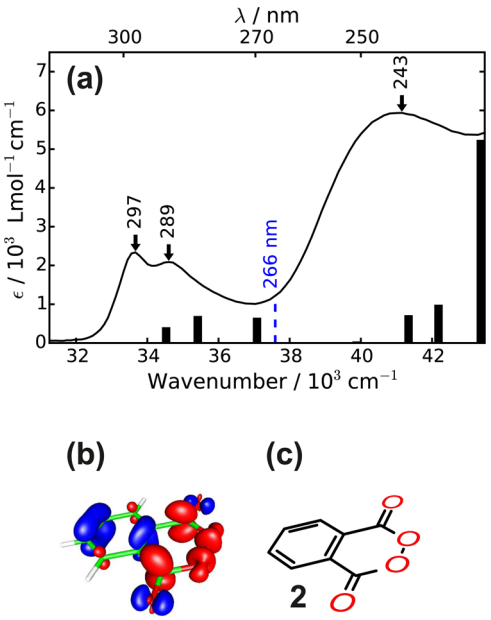

Figure 1. (a) Electronic spectrum of phtaloyl peroxide **2** in acetonitrile. The solid curve represents the experimental data. Absorption maxima are indicated by the arrows. The bars represent the electronic spectrum as calculated using TDDFT (see text for details). The blue dashed line at 266 nm represents the wavelength of the laser employed for photolysis. (b) Three dimensional plot corresponding to the electron-density shift induced by the 266 nm laser excitation. (c) Lewis structure of **2** with the same orientation as that used for the difference electron density representation.

low energy region features two partially resolved absorptions peaking at 297 and 289 nm and the high energy region a much broader band with a maximum at 243 nm. For understanding the underlying nature of those electronic transitions, time-dependent density functional theory (TDDFT) was employed. The solid bars in Figure 1a represent the BP86/def2-aug-TZVPP-TDDFT calculated electronic spectrum of **2** in which solvent effects were considered. As anticipated, the lowest energy transition, peaking at 297 nm, is mainly of HOMO → LUMO character, whereas its neighbor band at 289 nm is mostly the result of a HOMO-2 → LUMO transition (for details, see the Supporting Information). Interestingly, the TDDFT calculation shows that, close to the excitation wavelength (blue dashed line, Figure 1a), there is a transition that is mainly of HOMO-1 → LUMO character, although it contains contributions of higher energy excitations. To take into account the contribution of the complete set of individual excitations to the final electronic state, the difference of electron-density between the initial and final states requires consideration. Figure 1b shows the difference electron density plot for the transition most resonant with the 266 nm wavelength together with the Lewis structure of **2** for better visualization. The blue and red regions in the difference electron density plot represent negative and positive values, respectively. The electron density plot suggests that, upon 266 nm laser excitation, electron density from ring-π electrons is transferred directly into the carbonyl carbon atoms and oxygen atoms of the peroxide unit simultaneously. One can anticipate that the simultaneous allocation of electron density on the CO_2 moieties in **2** might induce their desired coherent photodissociation, leading to **1**.

2. Rapid-Scan Time-Resolved FTIR Spectroscopy. Figure 2a shows the FTIR absorption spectrum of CO_2 in

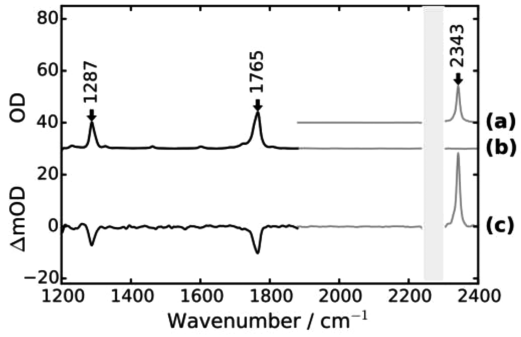

Figure 2. (a) Scaled and shifted FTIR spectrum of CO_2 in CH_3CN. (b) Scaled and shifted FTIR spectrum of **2** in CD_3CN (black) and CH_3CN (gray). (c) Difference absorption spectrum recorded 100 ms after 266 nm pulse excitation of the sample of **2** in Ar-purged CD_3CN (black) and CH_3CN (gray).

acetonitrile in the spectral region from 1900 to 2400 cm^{-1}. The strongest IR absorption of CO_2 peaks at 2343 cm^{-1} as indicated by the arrow. Figure 2b illustrates the scale and shifted FTIR absorption spectrum of **2** recorded in deuterated (black curve) and nondeuterated (gray curve) acetonitrile to circumvent the lack of IR transparency of acetonitrile in the region from 1350 to 1600 cm^{-1}. The strongest absorptions of **2** are located at 1287 and 1765 cm^{-1}. A normal-mode analysis conducted at the B3LYP/TZVP level of theory indicates that the 1287 cm^{-1} absorption is due to the coupling of ring stretching and in-plane bending of the C−H and C═O bonds along the entire molecule, whereas the 1765 cm^{-1} is the result of out-of-phase and in-phase stretching combinations of both C═O groups in **2**. Figure 2c shows a representative time-resolved difference FTIR absorption spectrum recorded 100 ms after 266 nm pulse excitation of **2** in acetonitrile under an inert argon atmosphere. The bands pointing downward arise from the increased transmission in the spectral region where **2** strongly absorbs and indicates its clean photolysis. Concomitantly, a new strong band at 2343 cm^{-1} due to CO_2 appears (compare to Figure 2a). The temporal formation of this band cannot be resolved with the limited time resolution of our rapid-scan FTIR setup (~60 ms).

Remarkably, there is no formation of IR absorption bands in the regions around 1287 and 1765 cm^{-1}, where **2** strongly absorbs. The absence of pump-induced absorptions around 1765 cm^{-1}, where carbonyl-containing compounds significantly absorb, is a strong indication that **2** is efficiently photoconverted to **1** and 2 equiv of CO_2 (path a, Scheme 3) in a

DOI: 10.1021/acs.joc.5b02678
J. Org. Chem. 2016, 81, 1151−1156

Scheme 3. Photolysis at 266 nm of 2 in Liquid Acetonitrile at Room Temperature

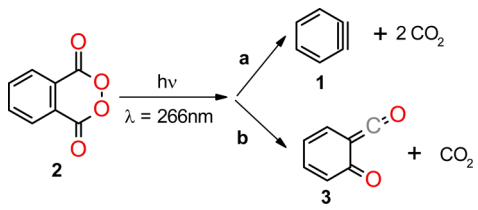

single photon process. Furthermore, bands around 1287 cm^{-1} due to photoproducts are expected to be less intense than that of parent **2** because the coupling mechanism with the C═O oscillators is no longer operating and they might well be buried in the baseline noise.

Organic reactive intermediates usually have lifetimes on the microsecond time scale and therefore the temporal resolution that rapid-scan FTIR spectroscopy provides is insufficient. In the next section, to circumvent the intrinsic temporal limitations of rapid-scan FTIR spectroscopy on the one hand and to establish the presence of elusive intermediates in the photolysis of **2** on the other, photolysis experiments on **2** monitored with nanosecond temporal resolution are described.

3. Step-Scan FTIR Spectroscopy. Representative step-scan time-resolved difference absorption spectra recorded 200 ns (red), 4 μs (orange), 16 μs (green), and 80 μs (blue) after the absorption of a single 266 nm laser pulse by **2** in liquid acetonitrile are illustrated in Figure 3a. All transient spectra

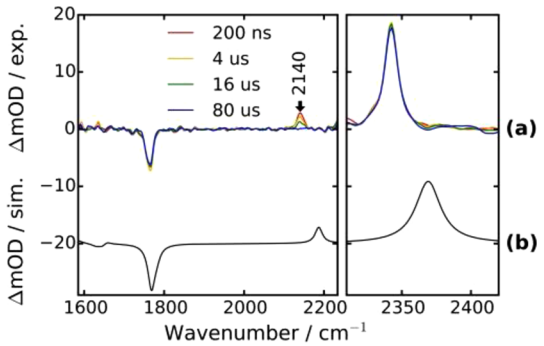

Figure 3. (a) Step-scan FTIR difference absorption spectra recorded for 200 ns (red), 4 μs (orange), 16 μs (green), and 80 μs (blue) after 266 nm laser-pulsed photolysis. The arrow indicates the spectral evolution of the transient IR absorption band with time. (b) DFT simulation of the 200 ns transient absorption spectrum (see text for details).

show a negative absorption at 1767 cm^{-1}, indicating the net photolysis of **2** and a gigantic positive absorption at 2343 cm^{-1} due to the simultaneous generation of CO_2. Even at the shortest delay time, 200 ns, both the transient depletion of **2** and the formation of CO_2 measured by their corresponding IR resonances are in their corresponding stationary values, indicating that the primary process leading to the actual dissociation of CO_2 from **2** and its thermal equilibration occur in time scales well below those accessible by the step-scan spectrometer. In contrast with the rapid-scan experiments, the step-scan difference absorption spectra show a previously undetected transient absorption at 2140 cm^{-1}. The species responsible for the 2140 cm^{-1} absorption reacts following a (pseudo)first-order kinetic law with a time constant of 22.5 μs, and 80 μs after the laser excitation, it is no longer detectable (blue spectrum, Figure 3a). A careful analysis performed on a large set of experimental data shows there is an additional weak absorption at 1636 cm^{-1} that decays with a time constant equal to that measured for the 2140 cm^{-1} absorption. The absorptions at 1636 cm^{-1} (carbonyl) and 2140 cm^{-1} (ketene) are ascribed to 6-oxocyclohexa-2,3-dienylideneketene (**3**). This assignment is supported by the similarity to the IR absorptions (1650 and 2139 cm^{-1}) of **3** isolated in inert cryogenic matrices.[31,32] Also, Liu et al.[33] generated **3** by 308 nm laser photolysis of 2-phenyl-3,1-benzoxan-4-one in acetonitrile at room temperature and observed a transient absorption at 2135 ± 2 cm^{-1} that decayed following first-order kinetics in the microsecond time scale. Furthermore, the transient absorptions of **3** are readily quenched if methanol is added to the acetonitrile solution before photolysis.

The step-scan experiments suggest there are two competing mechanisms in the photolysis of **2**. On the one hand, the resonance photoejection of two CO_2 molecules from **2** leads to the desired formation of **1** (path a, Scheme 3), and on the other hand, the ejection of a single CO_2 molecule from **2** leads to the ultimate formation of **3** (path b, Scheme 3). For quantification of the proportions of these competing photodissociation pathways, spectral simulations were carried out. Figure 3b shows the simulated transient spectrum at 200 ns using the theoretical IR spectra of the species **1**–**3** and CO_2 obtained from DFT (B3LYP/TZVP) calculations (for details, see SI). In the simulation, an 80% yield of **1** and a 20% yield of **3** is assumed. The nice agreement between experiment and theory suggests that the 266 nm photolysis of **2** in acetonitrile is a feasible route to **1** in liquid solution.

The limited time-resolution (200 ns) of the step-scan spectrometer does not allow one to resolve the formation of **3**. The formation of **3** can take place by incomplete photodecarboxylation of **2** coupled with an oxygen atom transfer (path b, Scheme 3). This incomplete photodecarboxylation pathway might occur in an excited or a ground potential energy surface with or without benzopropiolactone **4** as reactive intermediate. Alternatively, **1** could react with CO_2 (in cage), leading to **3** with **4** as a reactive intermediate (Scheme 4).

Scheme 4

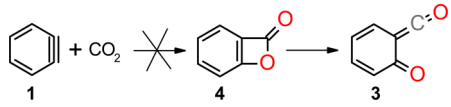

If the latter pathway is operating, conducting the photolysis in a CO_2 atmosphere should enhance the formation of **4** and **3**. The CO group in **4** gives rise to a strong IR resonance at 1904 cm^{-1} in Ar matrices at 8 K.[31] Therefore, the presence of **4** could be readily observed in the time-resolved FTIR experiments. Furthermore, DFT calculations suggest the transformation **4** → **3** is exergonic (ΔG = −9.0 kcal/mol), but it is hampered by a thermal barrier of 5.4 kcal/mol. For establishing whether **1** reacts with CO_2 leading to the ultimate formation of **3**, the step-scan experiments on **2** were carried out in CO_2 atmosphere. These experiments showed that the yield of **3** is unaffected by the presence of CO_2 in the reacting system, and therefore **3** should be formed directly from **2** by incomplete photodecarboxylation. Because the absorptions

DOI: 10.1021/acs.joc.5b02678
J. Org. Chem. 2016, 81, 1151−1156

bands of **4** were not detected, it can be concluded that **1** does not react with CO_2 in liquid acetonitrile.

For further investigation of the possible participation of elusive radical intermediates in the formation of **3**, independent step-scan experiments were carried out in the presence of molecular oxygen. Surprisingly, the time-resolved difference absorption spectra obtained in this way were formally identical to those obtained in experiments under inert argon atmosphere, which strongly suggests there are no radical intermediates on the pathway leading to **3**. From the body of these time-resolved FTIR experiments, one can conclude that the primary mechanistic steps leading to **3** occur on time scales shorter than those available to the step-scan regime (<200 ns).

Before closing this section, it is necessary to clarify why **1** is not directly observed in the nanosecond time-resolved FTIR experiments. The distinctive IR absorption of **1**, that is the C≡C stretching, peaks at 1846 cm^{-1} in Ne matrices at 4 K.[23] However, this absorption is extremely weak and therefore, as expected, is not observed in the step-scan time-resolved FTIR experiments. Other absorptions bands of **1** in the IR window available in the experimental setup (1050−2800 cm^{-1}) include ring stretchings with or without C−H bending contributions, which are also too weak to be detected or masked by other product absorptions. Therefore, for finally establishing the presence of **1** in the 266 nm photolysis of **2** in acetonitrile at room temperature, appropriate trapping experiments are mandatory. In the next section, the necessary trapping experiments on **1** that give rise to detectable IR spectral changes are described.

4. Quenching Experiments. In neat solvent, **1** dimerizes forming biphenylene **5** (path a, Scheme 5).[34,35] The IR spectrum of authentic samples of **5** in acetonitrile shows resonances at 1130, 1151, and 1261 cm^{-1}. The characteristic IR bands of **5** could not be clearly observed in the time-resolved FTIR experiments, presumably due to their intrinsic weakness (ε < 300 L $mol^{-1}cm^{-1}$), the insufficient signal-to-noise ratio, or because they might be simply masked by other product bands. At any rate, this channel is clearly invisible in our experiments and cannot account for the presence of **1**.

Scheme 5. Trapping Experiments on 1

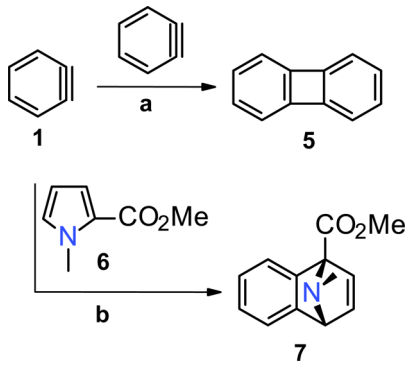

The strategy to confirm the presence of **1** requires an efficient trapping reaction easy to follow by IR spectroscopy. Strong nucleophiles such as N_3^-, SCN^-, and NCO^- were considered first. These quenchers are strong IR chromophores and are practically transparent to 266 nm light; however, they react readily with **2** leading to the instantaneous formation of phtaloyl anhydride. Therefore, they had to be disqualified as trapping reagents. Alkyl azides such as octyl azide[36] and **2** form acetonitrile solutions that are stable for indefinite periods of time. Octyl azide is photo inert to 266 nm laser light; however, the much anticipated [3 + 2] cycloaddition[16] reaction with **1** does not take place in acetonitrile solvent. DFT calculations suggest the [3 + 2] cycloaddition between **1** and alkyl azides is hampered by a significant thermal barrier.[21] However, it is important to point out that [3 + 2] cycloadditions between **1** and azides have been conducted via photolysis of **2** in dichloroethane solvent at room temperature.[16] Conducting the photolysis of **2** in CO-saturated acetonitrile gives rise to experimental data that is identical to that obtained when experiments are carried out in Ar atmosphere, thus confirming that a reaction between **1** and CO giving rise to benzocyclopropenone requires activation.[37]

Inspired by the quenching experiment on **1** with furan at 50 K in an argon matrix by Chapman,[22] I decided to use the Diels−Alder reactivity of **1** as a probe of its presence. For enhancement of the IR sensitivity of the corresponding Diels−Alder reaction, methyl 1-methylpyrrole-2-carboxylate (**6**) was selected. This quencher has the benefit of containing a built-in IR-CO chromophore whose temporal detection along the quenching reaction should in principle be feasible. It can be anticipated that the CO stretching frequency should shift to higher frequencies in the Diels−Alder adduct **7** with respect to that in **6** due to the missing conjugation in the final product. Compound **6** has the disadvantage that its UV−vis spectrum has a sharp maximum at 267 nm, which is very close to the excitation wavelength. Because the opacity of quencher **6** is high at 266 nm, "background" flash photolysis experiments on **6** alone in acetonitrile were carried out. The laser energy used in the photolysis experiments with **6** alone was at least equal to that employed in similar experiments with **2**. Under these experimental conditions, **6** does not undergo net photolysis, which means all photoexcited molecules of **6** return back to the ground state without experiencing any chemical transformation. Having established **6** is resistant to the action of 266 nm laser light, laser flash experiments with acetonitrile solutions of **2** and **6** (2:1) were carried out. Because of the inconvenient absorption of 266 nm laser light by **6**, the step-scan difference absorption spectra are significantly perturbed by thermal artifacts. Therefore, the millisecond rapid-scan time-resolved technique was the only alternative left to circumvent these experimental issues (a rapid-scan experiment requires approximately 16 laser shots; a step-scan experiment requires approximately 10600 laser shots).

The scaled and shifted IR spectra of **2** alone, and a mixture of **2** and **6** (2:1) in acetonitrile, are illustrated in Figure 4a. The IR absorption band of **2** at 1710 cm^{-1} is clearly resolved from that of **6** at 1765 cm^{-1}. Figure 4b illustrates the transient difference absorption spectrum recorded 100 ms after exciting with a 266 nm laser pulse, an acetonitrile solution containing **2**, and quencher **6**. The 100 ms difference absorption spectrum shows a photoinduced strong positive absorption band at 2343 cm^{-1} due to CO_2 formation, indicating the successful decarboxylation of **2** under these experimental conditions and negative absorptions at 1710 and 1765 cm^{-1}, indicating that both **6** and **2** undergo net photolysis. In addition, the 100 ms rapid-scan difference absorption spectrum shows a weak positive absorption at 1731 cm^{-1} (asterisk, Figure 4b). Although weak, the 1731 cm^{-1} absorption is reproducible on an experiment-to-experiment basis. For better understanding of the results of these rapid-scan experiments, the transient spectrum at 100 ms was simulated using the calculated IR spectra of the species

DOI: 10.1021/acs.joc.5b02678
J. Org. Chem. 2016, 81, 1151−1156

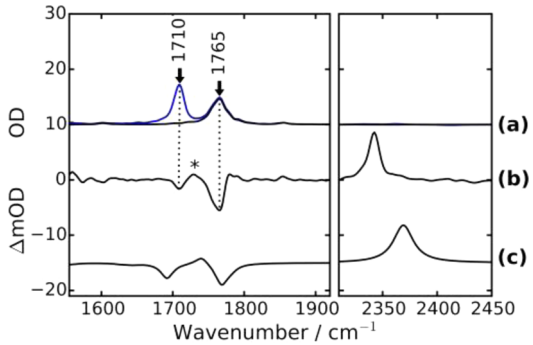

Figure 4. Quenching benzyne **1** with **6**. (a) Black: scaled and shifted FTIR spectrum of **2**. Blue: scaled and shifted FTIR spectrum of a solution containing **2** and **6** (2:1). (b) Difference absorption spectrum recorded 100 ms after 266 nm laser photolysis of a sample solution containing **2** and **6** in a molar ratio of 2:1. The asterisk marks the IR absorption of the reaction product between **1** and **6**. (c) A simulation of the difference absorption spectrum illustrated in (b) using the DFT theoretical IR spectra of all of the species involved (see text for details).

involved in this quenching experiment (path b, Scheme 5). Figure 4c shows the result of such a simulation (see Supporting Information). The excellent agreement between experiment and theory is very gratifying and indicates the quenching of **1** was finally successful.

An upper bound for the photolytic yield of **1** can be calculated from the magnitudes of the negative absorptions of precursor **2** (5.57 mOD) and quencher **6** (1.65 mOD) at 1708 and 1768 cm^{-1}, respectively (Figure 4b). Now, taking into account the extinction coefficients of **6** and **2** at the peak of the CO stretching maxima, they are equal to 0.76 and 1.93×10^3 L mol^{-1} cm^{-1}, respectively. The desired limiting yield for the formation of **1** is 75%. In the previous section, an 80% yield was calculated based on DFT simulated time-resolved step-scan FTIR spectra. It is remarkable that both calculated photolytic yields agree. This coincidence suggests the DFT calculated IR spectra can be employed for quantitative estimation and simulation of time-resolved FTIR spectra. Previous synthetic work has shown that Diels–Alder reactions with **1** are quantitative.[19] The experiments presented here confirm the synthetic findings. Before closing this section, I would like to mention that when methyl furan-2-carboxylate is employed as a quencher similar results are obtained, indicating that Diels–Alder reactions provide a convenient way to trap **1** in liquid acetonitrile.

CONCLUSIONS

o-Benzyne **1** has found numerous synthetic applications; however, real-time mechanistic studies on **1** in liquid solution are scarce and restricted to low-temperature conditions. I have confirmed that phtaloyl peroxide **2** is a suitable precursor of **1** in liquid acetonitrile solution when irradiated with 266 nm laser light. Reactant **1** is formed after the simultaneous loss of two CO_2 molecules from **2**, a process that cannot be temporally resolved with a step-scan FTIR spectrometer. In another competing, but less efficient, photolytic pathway, **2** ejects a single CO_2 molecule, and ketoketene **3** is formed. As expected, **3** reacts readily with methanol. The existence of **1** was confirmed by means of its Diels–Alder reactivity with 1-methylpyrrole-2-carboxylate **6**.

I am currently engaged in the application of the current protocol to asymmetric derivatives of **2** with the intention of detecting arynes in solution directly using time-resolved IR spectroscopy.

EXPERIMENTAL SECTION

General Methods. Acetonitrile was obtained from a commercial supplier, and it was stored for at least 2 days under molecular sieves (3 Å) prior to use. Phtaloyl peroxide was prepared according to a literature method.[38] Biphenylene and methyl 1-methylpyrrole-2-carboxylate were purchased from commercial providers and used as supplied.

Step-Scan Time-Resolved FTIR. Our step-scan instrument has been described elsewhere;[39] therefore, only a brief description is presented here. Stock solutions (250 mL) of phtaloyl peroxide (1–3 mmol L^{-1}) were circulated through a CaF_2 cell (0.2 mm path length) by means of a peristaltic pump. Photolysis took place inside the probe chamber of the step-scan spectrometer by the fourth harmonic pulses (266 nm, 7 ns) of a Nd:YAG laser. For avoiding thermal artifacts in the transient spectra, the energy of the 266 nm pulses was attenuated to 7 mJ/pulse before the sample cell. For circumventing extended irradiation times, the measurements were conducted with 6 cm^{-1} spectral resolution.

DFT Calculations. DFT calculations were performed with ORCA.[40] Geometry optimizations were carried out in two stages to obtain the best compromise between accuracy and computing time. In the first stage, the Becke–Perdew functional BP86[41,42] was used in conjunction with the Ahlrichs-VDZ[43,44] basis sets by invoking the resolution of the identity (RI)[45] approximation. In the second stage, the geometric parameters, previously obtained, were further refined using the hybrid B3LYP[46,47] functional in conjunction with the Ahlrichs-TZVP[44] basis set by invoking the RIJCOSX[48] approximation. Solvent effects were taken into account through the conductor-like screening model (COSMO).[49,50] For characterizing the nature (minimum or saddle point) of the optimized geometries, numerical frequencies were computed by two-sided numerical differentiation using step increments of 0.002 bohr.

The electronic spectra were calculated within the framework of the time-dependent density functional theory (TDDFT).[51,52] The first 16 excited states were computed using the BP86 functional in conjunction with the def2-aug-TZVPP[53] basis sets.

ASSOCIATED CONTENT

Supporting Information

The Supporting Information is available free of charge on the ACS Publications website at DOI: 10.1021/acs.joc.5b02678.

Cartesian coordinates and electronic energies for **1**–**7** and the transition structure for the transformation of **4** toward **3**, details of the calculated electronic spectrum of **2** by TDDFT, brief description of the methodology to simulate the difference time-resolved FTIR spectra, kinetic profiles at 2140 and 2343 cm^{-1} corresponding to step-scan experiments on **2** under inert argon atmosphere, and step-scan difference absorption FTIR spectra conducted on **2** in CO and O_2 atmospheres and with added methanol in argon-saturated acetonitrile (PDF)

AUTHOR INFORMATION

Corresponding Author

*E-mail: joel.torresalacan@pc.uni-bonn.de.

Notes

The authors declare no competing financial interest.

DOI: 10.1021/acs.joc.5b02678
J. Org. Chem. 2016, 81, 1151–1156

■ ACKNOWLEDGMENTS

Financial support by the Deutsche Forschungsgemeinschaft through the Collaborative Research Center "Chemistry at Spin Centers" is gratefully acknowledged.

■ REFERENCES

(1) Bachmann, W. E.; Clarke, H. T. *J. Am. Chem. Soc.* **1927**, *49*, 2089.
(2) Wittig, G. *Naturwissenschaften* **1942**, *30*, 696.
(3) Wittig, G.; Pohmer, L. *Angew. Chem.* **1955**, *67*, 348.
(4) Roberts, J. D.; Simmons, H. E.; Carlsmith, L. A.; Vaughan, C. W. *J. Am. Chem. Soc.* **1953**, *75*, 3290.
(5) Heaney, H. *Chem. Rev.* **1962**, *62*, 81.
(6) Wenk, H. H.; Winkler, M.; Sander, W. *Angew. Chem., Int. Ed.* **2003**, *42*, 502.
(7) Wentrup, C. *Aust. J. Chem.* **2010**, *63*, 979.
(8) Leopold, D. G.; Miller, T. M.; Lineberger, W. C. *J. Am. Chem. Soc.* **1986**, *108*, 178.
(9) Wenthold, P. G.; Squires, R. R.; Lineberger, W. C. *J. Am. Chem. Soc.* **1998**, *120*, 5279.
(10) Orendt, A. M.; Facelli, J. C.; Radziszewski, J. G.; Grant, D. M.; Michl, J. *J. Am. Chem. Soc.* **1996**, *118*, 846.
(11) Mclain, S. J.; Schrock, R. R.; Sharp, P. R.; Churchill, M. R.; Youngs, W. J. *J. Am. Chem. Soc.* **1979**, *101*, 263.
(12) Buchwald, S. L.; Watson, B. T.; Huffman, J. C. *J. Am. Chem. Soc.* **1986**, *108*, 7411.
(13) Buchwald, S. L.; Nielsen, R. B. *Chem. Rev.* **1988**, *88*, 1047.
(14) Stiles, M.; Miller, R. G.; Burckhardt, U. *J. Am. Chem. Soc.* **1963**, *85*, 1792.
(15) Jones, M.; Decamp, M. R. *J. Org. Chem.* **1971**, *36*, 1536.
(16) Chang, D.; Zhu, D.; Shi, L. *J. Org. Chem.* **2015**, *80*, 5928.
(17) Bennett, M. A.; Wenger, E. *Chem. Ber.* **1997**, *130*, 1029.
(18) Pellissier, H.; Santelli, M. *Tetrahedron* **2003**, *59*, 701.
(19) Kitamura, T.; Yamane, M. *J. Chem. Soc., Chem. Commun.* **1995**, 983.
(20) Tadross, P. M.; Stoltz, B. M. *Chem. Rev.* **2012**, *112*, 3550.
(21) Medina, J. M.; Mackey, J. L.; Garg, N. K.; Houk, K. N. *J. Am. Chem. Soc.* **2014**, *136*, 15798.
(22) Chapman, O. L.; Mattes, K.; McIntosh, C. L.; Pacansky, J.; Calder, G. V.; Orr, G. *J. Am. Chem. Soc.* **1973**, *95*, 6134.
(23) Radziszewski, J. G.; Hess, B. A., Jr.; Zahradnik, R. *J. Am. Chem. Soc.* **1992**, *114*, 52.
(24) Scheiner, A. C.; Schaefer, H. F.; Liu, B. *J. Am. Chem. Soc.* **1989**, *111*, 3118.
(25) Berry, R. S.; Stiles, M.; Spokes, G. N. *J. Am. Chem. Soc.* **1962**, *84*, 3570.
(26) Diau, E. W. G.; Casanova, J.; Roberts, J. D.; Zewail, A. H. *Proc. Natl. Acad. Sci. U. S. A.* **2000**, *97*, 1376.
(27) Warmuth, R. *Angew. Chem., Int. Ed. Engl.* **1997**, *36*, 1347.
(28) Bucher, G.; Halupka, M.; Kolano, C.; Schade, O.; Sander, W. *Eur. J. Org. Chem.* **2001**, *2001*, 545.
(29) Colley, C. S.; Grills, D. C.; Besley, N. A.; Jockusch, S.; Matousek, P.; Parker, A. W.; Towrie, M.; Turro, N. J.; Gill, P. M. W.; George, M. W. *J. Am. Chem. Soc.* **2002**, *124*, 14952.
(30) Torres-Alacan, J.; Vohringer, P. *Int. Rev. Phys. Chem.* **2014**, *33*, 521.
(31) Chapman, O. L.; McIntosh, C. L.; Pacansky, J.; Calder, G. V.; Orr, G. *J. Am. Chem. Soc.* **1973**, *95*, 4061.
(32) Koch, R.; Blanch, R. J.; Wentrup, C. *J. Org. Chem.* **2014**, *79*, 6978.
(33) Liu, R. C. -Y.; Lusztyk, J.; McAllister, M. A.; Tidwell, T. T.; Wagner, B. D. *J. Am. Chem. Soc.* **1998**, *120*, 6247.
(34) Logullo, F. M.; Seitz, A. H.; Friedman, L. *Org. Synth.* **1968**, *48*, 12.
(35) Dvorak, V.; Kolc, J.; Michl, J. *Tetrahedron Lett.* **1972**, *13*, 3443.
(36) Alvarez, S. G.; Alvarez, M. T. *Synthesis* **1997**, *1997*, 413.
(37) Simon, J. G. G.; Munzel, N.; Schweig, A. *Chem. Phys. Lett.* **1990**, *170*, 187.
(38) Yuan, C. X.; Axelrod, A.; Varela, M.; Danysh, L.; Siegel, D. *Tetrahedron Lett.* **2011**, *52*, 2540.
(39) Torres-Alacan, J.; Krahe, O.; Filippou, A. C.; Neese, F.; Schwarzer, D.; Vohringer, P. *Chem. - Eur. J.* **2012**, *18*, 3043.
(40) Neese, F. *ORCA-An ab Initio, Density Functional, and Semiempirical Program Package Version 2.8*; University of Bonn, Bonn, Germany, 2011.
(41) Perdew, J. P.; Yue, W. *Phys. Rev. B: Condens. Matter Mater. Phys.* **1986**, *33*, 8800.
(42) Becke, A. D. *Phys. Rev. A: At., Mol., Opt. Phys.* **1988**, *38*, 3098.
(43) Schafer, A.; Horn, H.; Ahlrichs, R. *J. Chem. Phys.* **1992**, *97*, 2571.
(44) Eichkorn, K.; Weigend, F.; Treutler, O.; Ahlrichs, R. *Theor. Chem. Acc.* **1997**, *97*, 119.
(45) Kendall, R. A.; Fruchtl, H. A. *Theor. Chem. Acc.* **1997**, *97*, 158.
(46) Lee, C. T.; Yang, W. T.; Parr, R. G. *Phys. Rev. B: Condens. Matter Mater. Phys.* **1988**, *37*, 785.
(47) Becke, A. D. *J. Chem. Phys.* **1993**, *98*, 5648.
(48) Neese, F.; Wennmohs, F.; Hansen, A.; Becker, U. *Chem. Phys.* **2009**, *356*, 98.
(49) Klamt, A.; Schuurmann, G. *J. Chem. Soc., Perkin Trans. 2* **1993**, 799.
(50) Klamt, A. *J. Phys. Chem.* **1995**, *99*, 2224.
(51) Gross, E. K. U.; Dobson, J. F.; Petersilka, M. *Density Functional Theory II* **1996**, *181*, 81.
(52) Dreuw, A.; Head-Gordon, M. *Chem. Rev.* **2005**, *105*, 4009.
(53) Weigend, F.; Ahlrichs, R. *Phys. Chem. Chem. Phys.* **2005**, *7*, 3297.

DOI: 10.1021/acs.joc.5b02678
J. Org. Chem. 2016, 81, 1151−1156